



# Thin films with implemented molecular switches for the application in polymer-based optical waveguides

Maximilian Seydi Kilic<sup>1</sup> · Jules Brehme<sup>1,2,3</sup> · Yves Deja<sup>4</sup> · Justus Pawlak<sup>1,3</sup> · Axel Günther<sup>4,5</sup> · Arthur Sander<sup>1</sup> · Dietrich Müller<sup>2</sup> · Antonia Renz<sup>1</sup> · Cyril Rajnak<sup>6</sup> · Michaela Polášková<sup>7</sup> · Bernhard Roth<sup>4,5</sup> · Ralf Franz Sindelar<sup>2,3</sup> · Franz Renz<sup>1,3</sup>

Accepted: 2 January 2024  
© The Author(s) 2024

## Abstract

Complexes like iron (II)-triazoles exhibit spin crossover behavior at ambient temperature and are often considered for possible application. In previous studies, we implemented complexes of this type into polymer nanofibers and first polymer-based optical waveguide sensor systems. In our current study, we synthesized complexes of this type, implemented them into polymers and obtained composites through drop casting and doctor blading. We present that a certain combination of polymer and complex can lead to composites with high potential for optical devices. For this purpose, we used two different complexes  $[\text{Fe}(\text{atrz})_3](2\text{ ns})_2$  and  $[\text{Fe}(\text{atrz})_3]\text{Cl}_{1.5}(\text{BF}_4)_{0.5}$  with different polymers for each composite. We show through transmission measurements and UV/VIS spectroscopy that the optical properties of these composite materials can reversibly change due to the spin crossover effect.

**Keywords** Spin crossover · Triazole complexes · Composite materials · Molecular switches · Waveguides · Polymers · Thin film

## 1 Introduction

Spin crossover materials are coordination compounds that can exhibit a reversible spin transition between high-spin and low-spin states of their centered metal ion. This transition is triggered by physical (temperature, pressure, light etc.) or chemical external influences and leads to a controllable change of the properties of these compounds [1, 2]. Coordination compounds that show this effect offer perspectives for several possible applications for example in the field of optical devices. The reversible switching between spin states with different physical features could enable novel optical sensor schemes as these compounds show a high sensitivity towards the formerly mentioned external stimuli [3]. Spin crossover compounds like Iron (II)-triazole complexes are often discussed for possible applications in different

---

Maximilian Seydi Kilic and Jules Brehme contributed equally to this work.

---

✉ Maximilian Seydi Kilic  
maximilian.kilic@acd.uni-hannover.de

Extended author information available on the last page of the article

fields. These complexes exhibit the spin crossover effect around room temperature as well as at lower and higher temperatures and are also sensitive to other influences [3–6]. The temperature range in which the effect can be observed depends on the choice of the respective ligands and anions. Thereby, anions and ligands can also be combined accordingly [1, 7]. In previous studies we implemented these complexes into first prototypes of polymer-based optical waveguides [8]. We were furthermore able to test the fabrication method of electrospinning to obtain polymer complex composite fiber mats with spin crossover properties and to prove that these complexes do not decompose under harsh conditions [9]. In order to find the optimal mixture between triazole complexes and polymers for the application in polymer-based optical waveguides, two different iron (II)-triazole complexes were implemented into polymer thin films. In the first approach, an insoluble complex was dispersed in a mixture with polystyrene then added to a petri dish and dried overnight. In the second approach a soluble iron (II)-triazole complex was used with 2-naphthalenesulfonate anions. A solution of the complex and polyacrylonitrile were doctor bladed on a glass surface and dried overnight. Both samples were thin films and showed visible optical changes in transmission by heating. Mössbauer spectroscopy was used to prove the successful implementation of the complexes into the polymers and to further investigate if the complexes oxidized during the process. The optical properties were investigated by using a laser device, UV/VIS spectroscopy and magnetic measurements. Our results give prove to a successful implementation and suggest that the obtained composites may be useful for the application in polymer-based optical waveguides suitable for sensing applications.

## 2 Materials and methods

### 2.1 Materials

The used Fe (II)-triazole complexes and composite materials were synthesized by using the following purchased chemicals without further purifying them: Iron(II)-Chloridetetrahydrate ( $\text{FeCl}_2 \cdot 4\text{H}_2\text{O}$ ) (>99%) from Sigma-Aldrich (St. Louis, MO, USA); L-Ascorbic acid (>99%) from Carl Roth; 4-Amino-1,2,4-Triazole (99%) purchased from Thermo Scientific (Waltham, MA, USA); Iron(II)-Tetrafluoroborate hexahydrate from Sigma-Aldrich (Sr. Louis, MO, USA); Sodium 2-Naphthalenesulfonate (98%) from Alfa Aesar (Haverhill, MA, USA); polyacrylonitrile (PAN) 150,000Mw and Polystyrene (PS) from Sigma-Aldrich (St. Louis, MO, USA); and N,N-Dimethylformamide (DMF) from Carl Roth.

### 2.2 Characterization

Infrared spectroscopy was performed to gain information about the molecular structure of the complex, polymer and composite. For this, a Perkin Elmer Spectrum Two spectrometer was used the ATR method in the range between 500 and 4000  $\text{cm}^{-1}$ .

The UV/VIS was performed using a Lambda 650S from Perkin Elmer from 800 to 250 nm in 1 nm steps. The composite materials were placed in the reflectance sample holder of the 150 mm integrating sphere with a heater behind it to increase the temperature of the sample up to the spin transition, to determine if the spin transition occurs.

CNH elemental analysis was performed using a Perkin-Elmer 2400 II CNH analyzer. Mössbauer measurements were carried out in transmission geometry with a modified miniaturized Mössbauer Spectrometer MIMOS II (Space and Earth Science Instrumentation) at

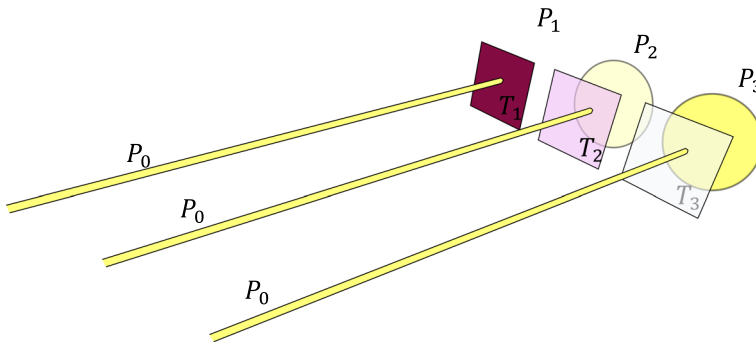


**Fig. 1** Schematic transmission measurements

room temperature. The measured Mössbauer spectra were recorded in transmission and the gamma radiation source consisted of  $^{57}\text{Co}$  nuclei in a Rh matrix. The measurements were recorded with 14.4 kV and all isomer shifts were given relative to  $\alpha\text{-Fe}$ .

Magnetic data was acquired with the help of the SQUID magnetometer (MPMS3, Quantum Design) at the vsm data taking modes. DC magnetic susceptibility was taken at BDC = 0.1 T (for all samples) and additionally in one case at BDC = 0.5 T (PAN foil with  $[\text{Fe}(\text{atrz})_3]\text{Cl}_{1.5}(\text{BF}_4)_{0.5}$  between 2 and 300 K (for  $[\text{Fe}(\text{atrz})_3]\text{Cl}_{1.5}(\text{BF}_4)_{0.5}$  and PS with  $[\text{Fe}(\text{atrz})_3]\text{Cl}_{1.5}(\text{BF}_4)_{0.5}$ , 2 and 340 K ( $[\text{Fe}(\text{atrz})_3]\text{Cl}_{1.5}(\text{BF}_4)_{0.5}$ ) and 2 and 400 K (PAN foil with  $[\text{Fe}(\text{atrz})_3](2\text{ ns})_2$ ).

To further homogenize one of the composite mixtures, a Fisherbrand Homogenizer 150 was used.

The transmission measurements were performed with an OXXIUS L6CC-CSB-2510 laser system and a THORLABS PM200 Touch Screen Power and Energy Meter Console. An adjustable power supply (VOLT CRAFT LRP-1363) and Peltier element (to heat the samples) were also used. A schematic of the transmission measurement is shown in Fig. 1.

An optical microscope (Primostar) by Zeiss was used to determine the film thickness of the obtained composites.

## 2.3 Methods

### 2.3.1 Synthesis of $[\text{Fe}(\text{atrz})_3]\text{Cl}_{1.5}(\text{BF}_4)_{0.5}$

The synthesis was performed according to a previously mentioned reaction of the pure chloride complex [9]. Therefore,  $\text{BF}_4$  anions were added in a stoichiometric ratio to decrease the occurring transition temperature. First 0.220 g  $\text{FeCl}_2 \cdot 4\text{H}_2\text{O}$  (1.110 mmol) and 0.1293 g of  $\text{Fe}(\text{BF}_4)_2 \cdot 6\text{H}_2\text{O}$  (0.383 mmol) were dissolved in 0.625 mL  $\text{H}_2\text{O}$  together with 20 mg of L-ascorbic acid. Separately 0.373 g 4-Amino-1,2,4-triazole (4.436 mmol) were also dissolved in 0.625 mL of  $\text{H}_2\text{O}$ . The iron(II) solution was then added to the triazole solution and then stirred at 600 rpm for 2 h and a white solid precipitated from the solution. The white solid was then washed three times with ethanol and centrifuged at 5000 rpm for 10 min each time. In the process, the obtained product became increasingly pink. It was then washed in chloroform and again centrifuged at 5000 rpm. The chloroform was then removed and the solid was dried overnight. 0.3912 g of a pink solid was obtained. (Yield: 65.31%) Analytically found (calculated) with CHN elemental analysis for  $\text{FeC}_6\text{H}_{12}\text{N}_{12}\text{B}_{0.5}\text{Cl}_{1.5} \cdot 2\text{H}_2\text{O}$  (molar

mass 440.697 g mol<sup>-1</sup>): C, 16.41 (16.35); H, 3.41 (3.66); N, 37.86 (38.14) MIR (in cm<sup>-1</sup>): 523 (s), 623 (s), 702 (m), 881 (m), 997 (s), 1025 (s), 1060 (s), 1097 (s), 1219 (s), 1294 (w), 1360 (w), 1398 (w), 1490 (w), 1545 (m), 1618 (m), 1663 (w), 2997 (m), 3065 (s), 3111(s), 3206 (m), 3264 (s), 3313 (m).

### 2.3.2 Dropcasting of PS with [Fe(atrz)<sub>3</sub>]Cl<sub>1.5</sub>(BF<sub>4</sub>)<sub>0.5</sub>

From the previously obtained complex, 125 mg were dispersed together with 400 mg polystyrene (PS) in 2.5 mL chloroform for one hour in an ultrasonic bath. The obtained suspension was then further treated with a homogenizer for 15 min. The resulting suspension was subsequently placed in a Petri dish via drop casting and allowed to dry overnight.

### 2.3.3 Synthesis of [Fe(atrz)<sub>3</sub>](2 ns)<sub>2</sub>

For the synthesis of [Fe(atrz)<sub>3</sub>](2 ns)<sub>2</sub> it was first necessary to synthesise the corresponding Fe (II)-salt Fe(2 ns)<sub>2</sub> · 6H<sub>2</sub>O. This was done as previously mentioned [9]. Therefore, 2.5 g of Sodium 2-Naphthalenesulfonate (10.85 mmol) were dissolved in 75 mL of H<sub>2</sub>O by heating up to 75° while stirring. A solution of 1.08 g of FeCl<sub>2</sub> · 4H<sub>2</sub>O (5.425 mmol) in 2.5 mL of H<sub>2</sub>O was then added to the Sodium 2-Naphthalenesulfonate solution. The solution was then stirred for 1 h and a white solid precipitated. The obtained solid was washed three times with 150 mL of water. The white solid was dried under vacuum in a desiccator overnight and 2.01 g were obtained. To confirm that the synthesis of Fe(2 ns)<sub>2</sub> · 6H<sub>2</sub>O was successful, IR spectroscopy was used. (Yield: 64.05 %) MIR (in cm<sup>-1</sup>): 612 (m), 621 (m), 645 (m), 668 (m), 736 (w, broad), 758 (s), 815 (s), 906 (w), 943 (w), 964 (w), 1033 (s), 1091 (m), 1181 (s, broad), 1347 (w), 1503 (m), 1592 (m), 1646 (s), 1670 (w), 1981 (w), 2364 (w, broad), 3061 (w), 3364 (s, broad).

Afterwards, the synthesis of the complex [Fe(atrz)<sub>3</sub>](2 ns)<sub>2</sub> was also done as previously mentioned [9]. Therefore, 1,4791 g of Fe(2 ns)<sub>2</sub> · 6H<sub>2</sub>O (2,369 mmol) were dissolved in 6 mL of methanol with 90 mg of ascorbic acid. Separately 0,6483 g of 4-amino-1,2,4-triazole (7,705 mmol) were dissolved in 5 mL of water. The iron(II)-salt containing solution was added to the triazole-solution and a pink solid precipitated. This product was then washed 3 times with ethanol and centrifugated for 10 min at 5000 rpm. The product was then dried overnight and 1,616 g were obtained. (Yield: 88.8 %) Analytically found (calculated) with CHN elemental analysis for FeC<sub>26</sub>H<sub>26</sub>N<sub>12</sub>O<sub>6</sub>S<sub>2</sub> · 4H<sub>2</sub>O (molar mass 794.597 g mol<sup>-1</sup>): C, 38.90 (39.30); H, 4.07 (4.31); N, 21.13 (21.15) (molar mass 766.49 g mol<sup>-1</sup>) C, 40.55 (40.74), H, 3.67 (4.06), N, 21.77 (21.93). IR 474 (m), 516 (m), 555 (s), 621 (s), 644 (m), 675 (s), 754 (s), 818 (s), 865 (s), 902 (s), 943 (m), 956 (m), 981 (w), 1032 (s), 1063 (m), 1092 (s), 1136 (s), 1171 (s), 1271 (s), 1346 (w), 1383 (w), 1446 (m), 1504 (w), 1547 (w), 1591 (w), 1625 (m,broad), 3011 (w), 3067 (m), 3073 (w), 3111 (w), 3163 (m), 3221 (w), 3283 (m,broad), 3498 (m,broad).

### 2.3.4 Doctorblading of PAN foil with [Fe(atrz)<sub>3</sub>](2 ns)<sub>2</sub>

A solution was prepared by solving 1.103 g PAN in 3 mL DMF and was stirred overnight for 12 h to obtain a homogeneous solution. A separate solution was prepared by solving 0.353 g [Fe(atrz)<sub>3</sub>](2 ns)<sub>2</sub> with 0.207 g L-Ascorbic acid in 7 ml DMF (*N,N*-Dimethylformamide) and sonicated for 1 h. Following that, both solutions were combined under heavy stirring. Parts of the solution were then poured on a glass plate and doctor bladed using a 200 μm distance

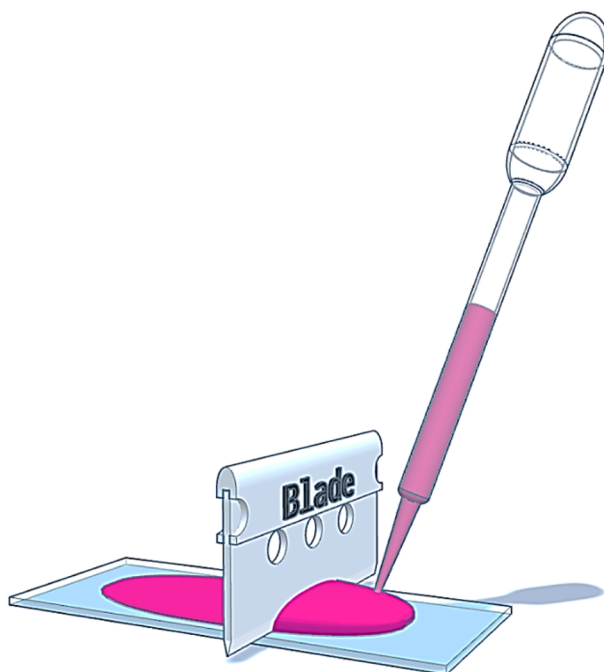


**Fig. 2** Scheme of the doctor blading applied to the suspension

(This process is shown in Fig. 2). Afterwards, the bladed solution was placed in an oven to dry at 80 °C before the purple thin films were collected.

### 3 Results

#### 3.1 $[\text{Fe}(\text{atrz})_3]\text{Cl}_{1.5}(\text{BF}_4)_{0.5}$ in PS

The Mössbauer spectra of the complex in Fig. 3 showed that the product had the majority of  $\text{Fe}^{\text{II}}$  in the LS state and partially  $\text{Fe}^{\text{II}}$  in the HS state. The product itself was supposed to be a mixed anionic  $\text{Fe}^{\text{II}}$ -triazole-complex. The isomeric shift and the quadrupole splitting in the measured Mössbauer spectrum in Fig. 3 are characteristic for  $\text{Fe}^{\text{II}}$ -triazole complexes and indicate a successful complex synthesis [4, 10].

The Mössbauer spectrum in Fig. 4 after the implementation of the complex into the PS also showed two different signals. These signals could also be assigned to a majority of  $\text{Fe}^{\text{II}}$  in the LS state and partially  $\text{Fe}^{\text{II}}$  in the HS state. However, an increase of the LS state population was observed. This indicates that a partial reaction between the polymer and the complex might have occurred. The measured Mössbauer parameters of the complex and the corresponding PCC are listed in Table 1 below.

The measured IR data of the product which was supposed to be a mixed-anionic triazole complex showed bonds that can be assigned to an  $\text{Fe}^{\text{II}}$ -triazole complexes. All significant bonds including the  $\text{BF}_4$ -bonds were visible. These were also slightly visible inside of the polymer complex composite (PCC). A direct comparison of the IR spectrum of the PCC,

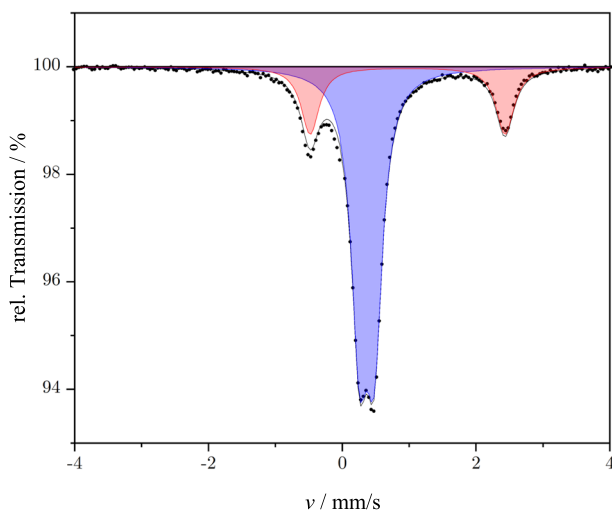


**Fig. 3** Mössbauer spectrum  $[\text{Fe}(\text{atrz})_3]\text{Cl}_{1.5}(\text{BF}_4)_{0.5}$  at 293 K, with two visible signals

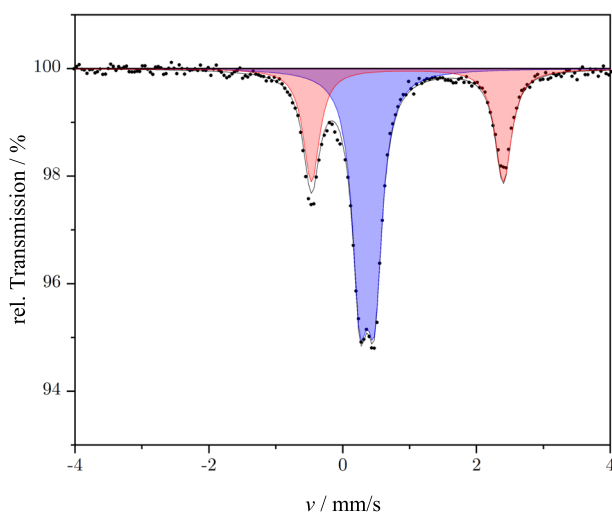


**Fig. 4** Mössbauer spectrum  $[\text{Fe}(\text{atrz})_3]\text{Cl}_{1.5}(\text{BF}_4)_{0.5}$  in PS at 293 K, with two visible signals

the complex, and PS is given in Fig. 5a. Significant bonds of the PS were also visible in the IR measurement of the PCC. This indicates a successful implementation of the obtained complex into the polymer.

Through the UV/VIS in Fig. 5b it is possible to see that the obtained complex and PCC both show an absorption maximum at 535 nm. This band further flattens in both cases after heating. This can be explained by the SCO behavior of the used complex.

To further analyze the SCO behavior, magnetic measurements were performed, shown in Fig. 6. The measured magnetic data of  $[\text{Fe}(\text{atrz})_3]\text{Cl}_{1.5}(\text{BF}_4)_{0.5}$  and  $[\text{Fe}(\text{atrz})_3]\text{Cl}_{1.5}(\text{BF}_4)_{0.5}$  in PS reveal that when the powder sample is added to the polymer matrix, the SCO behavior does not disappear, but the hysteresis loop narrows. The SCO compound has a characteristic

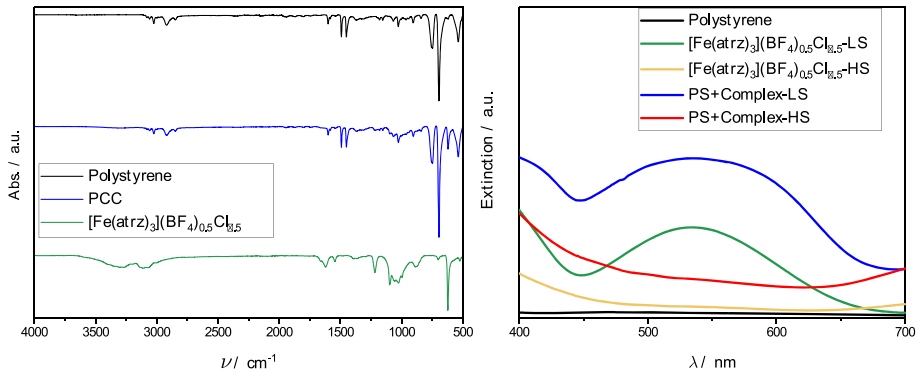


**Fig. 5** IR- (left) and UV/VIS-spectra (right) of pristine Polystyrene,  $[\text{Fe}(\text{atrz})_3]\text{Cl}_{1.5}(\text{BF}_4)_{0.5}$  and the composite. For the UV/VIS spectra, additional measurements at high temperatures (373 K) were performed

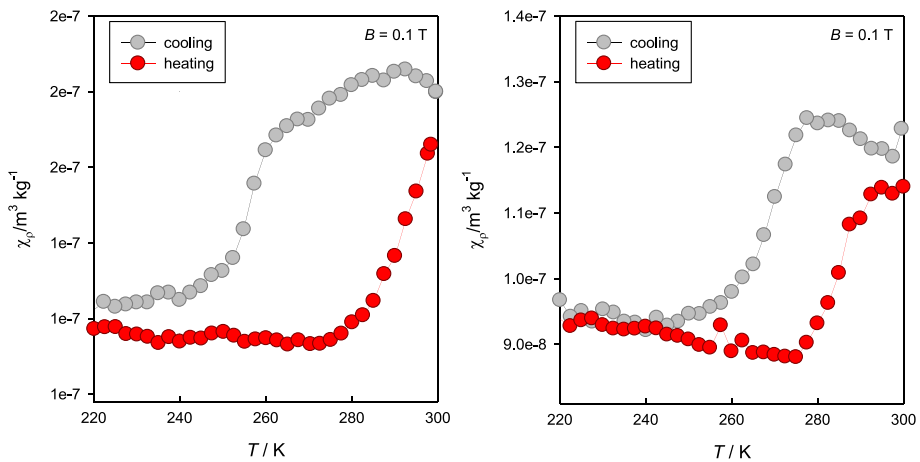


**Fig. 6** Magnetic measurements performed with a SQUID magnetometer. Pure complex  $[\text{Fe}(\text{atrz})_3]\text{Cl}_{1.5}(\text{BF}_4)_{0.5}$  shown on the left described by the magnetic susceptibility depending on temperature.  $[\text{Fe}(\text{atrz})_3]\text{Cl}_{1.5}(\text{BF}_4)_{0.5}$  in PS on the right represented by magnetic moment depending on temperature

pink color at room temperature and turns white due to the SCO at higher temperatures. The obtained PCC also had a pink color at ambient temperature but seems to be colorless and transparent after heating. This is why the change in the transmission of light (520 nm) during heating was additionally tested on the material. Through the spectrum in Fig. 7 it was possible to determine that the transmission increased from roughly 3% of the light to almost 15%. Thus, the transmission through the material has increased fivefold due to the spin crossover.

The thickness of the PCC was also further investigated by optical microscopy. An image is shown in Fig. 8. Through this it was possible to determine that the obtained PCC had a layer thickness of roughly 445  $\mu\text{m}$ .

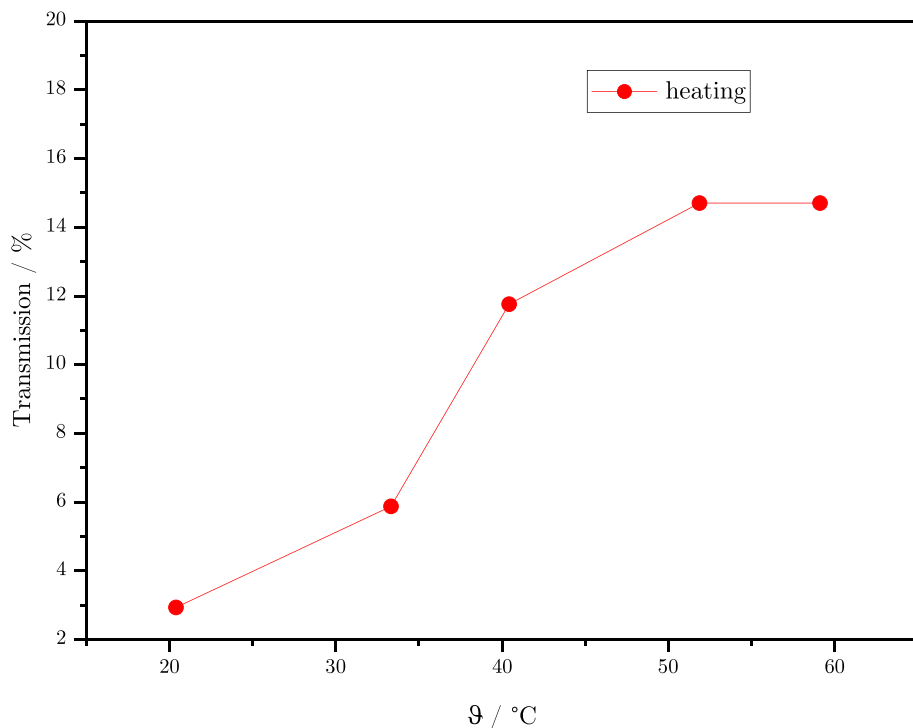


**Fig. 7** Transmission measurements of  $[\text{Fe}(\text{atrz})_3]\text{Cl}_{1.5}(\text{BF}_4)_{0.5}$  in polystyrene with varying temperatures

### 3.2 Thin film of $[\text{Fe}(\text{atrz})_3](2 \text{ ns})_2$ with PAN

The Mössbauer spectrum at room temperature in Fig. 9 showed that the obtained product only developed a single signal. This signal's isomeric shift and quadrupole splitting are characteristic for an  $\text{Fe}^{\text{II}}$ -triazole complex in the LS state [10]. This gave the indication of a successful synthesis of the complex.

In comparison to the literature of the known complex [11] our product only exhibited signals for Iron(II) in the LS state. This could on the one hand be explained by a different water content [10] in the sample and on the other hand that our product was three times purified with ethanol by centrifugation. Furthermore, the synthesis was carried out with different concentrations, resulting in different sizes of particles which can also have an influence on the SCO behaviour and spin state distribution.<sup>MSK</sup>

The corresponding Mössbauer spectrum after the implementation into PAN foil through doctor blading is shown in Fig. 10. Similar to the pure complex a single signal was observed. This signal had only minor differences in its isomeric shift and quadrupole splitting. Therefore, this signal was also characteristic for an  $\text{Fe}^{\text{II}}$ -triazole complex in the LS state.

The Mössbauer parameters of both spectra are shown in Table 1. By comparing the Mössbauer spectra before and after the implementation of the complex into the PAN, it can be expected that the implementation was successful and without side reactions. The slight change in the parameters can be explained by minor physical interactions of the polymer matrix and the complex. The comparison of the IR spectra of pure complex, pure PAN and the composite thin film in Fig. 11a also depicts that bonds of the complex and the polymer are visible in the





**Fig. 8** Microscopic image of  $[\text{Fe}(\text{atrz})_3]\text{Cl}_{1.5}(\text{BF}_4)_{0.5}$  in Polystyrene

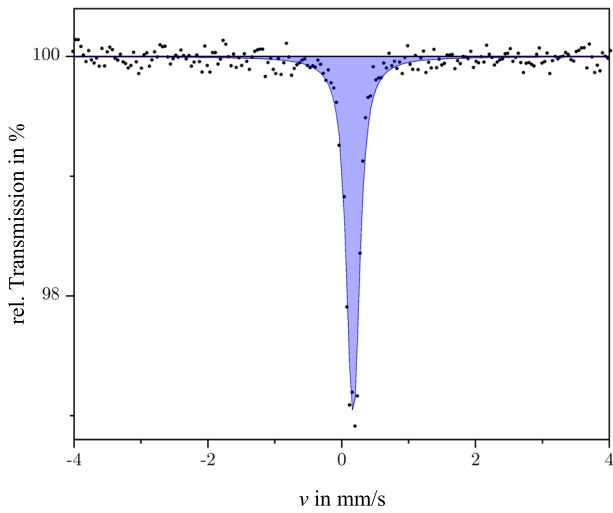


**Fig. 9** Mössbauer spectrum  $[\text{Fe}(\text{atrz})_3](2 \text{ ns})_2$  at 293 K, with one visible signal

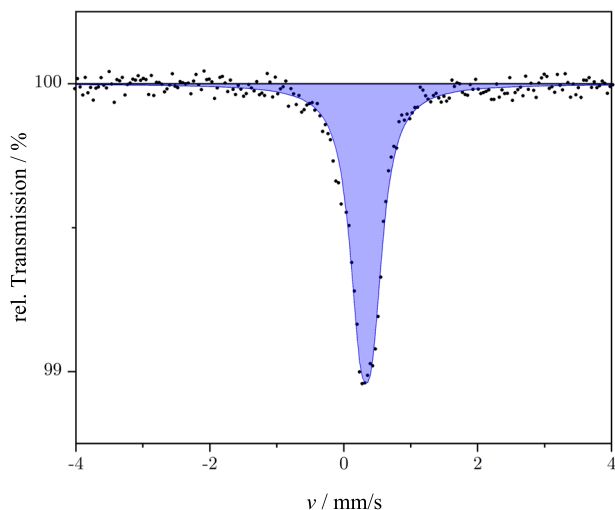


**Fig. 10** Mössbauer spectrum of PAN-[Fe(atrz)<sub>3</sub>](2 ns)<sub>2</sub>-foil at 293 K, with one visible signal

**Table 1** Mössbauer parameters of the discussed compounds at 293 K related to  $\alpha$ -Fe. Interpreted spin state taken from Varnek [5]

Sample	$\delta / \text{mm s}^{-1}$	$\Delta E_Q / \text{mm s}^{-1}$	$\Gamma/2 / \text{mm s}^{-1}$	Spin State	rel. area	Fig.
[Fe(atrz) <sub>3</sub> ]Cl <sub>1.5</sub> (BF <sub>4</sub> ) <sub>0.5</sub>	0.475	0.220	0.148	Fe <sup>II</sup> <sub>LS</sub>	77.13 %	3
	1.083	2.913	0.164	Fe <sup>II</sup> <sub>HS</sub>	22.86 %	
PS-[Fe(atrz) <sub>3</sub> ]Cl <sub>1.5</sub> (BF <sub>4</sub> ) <sub>0.5</sub>	0.474	0.214	0.139	Fe <sup>II</sup> <sub>LS</sub>	63.17 %	4
	1.074	2.867	0.148	Fe <sup>II</sup> <sub>HS</sub>	36.82 %	
[Fe(atrz) <sub>3</sub> ](2 ns) <sub>2</sub>	0.278	0.074	0.099	Fe <sup>II</sup> <sub>LS</sub>	100 %	9
PAN-[Fe(atrz) <sub>3</sub> ](2 ns) <sub>2</sub> -foil	0.440	0.185	0.199	Fe <sup>II</sup> <sub>LS</sub>	100 %	10

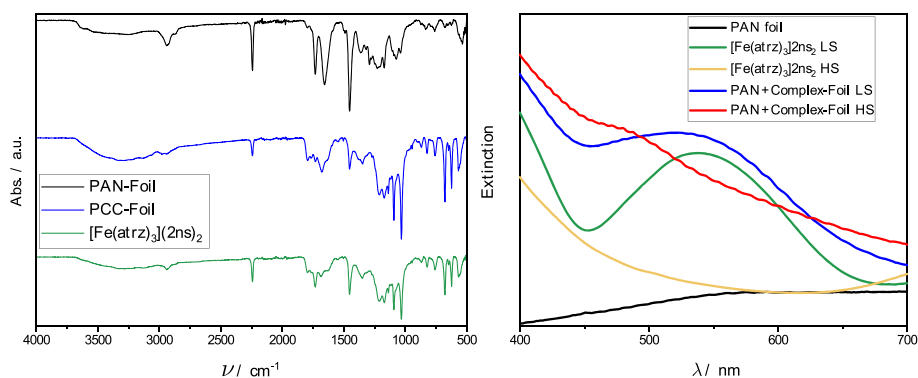


**Fig. 11** IR- (left) and UV/VIS-spectra (right) of pristine PAN, [Fe(atrz)<sub>3</sub>](2 ns)<sub>2</sub> and the composite. For the UV/VIS spectra, additional measurements at high temperatures (373 K) were performed

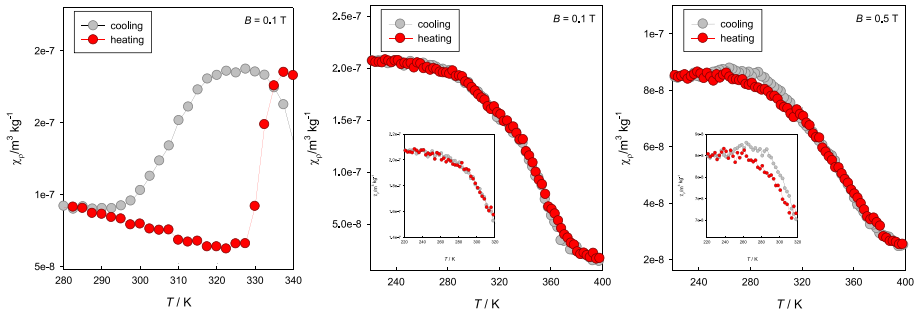


**Fig. 12** Magnetic measurements performed with a SQUID magnetometer. Pure complex  $[Fe(atrz)_3](2 ns)_2$  shown on the left described by the magnetic susceptibility depending on the temperature.  $[Fe(atrz)_3](2 ns)_2$  in PAN in the middle with 0.1 T and on the right with 0.5 T represented by magnetic moment depending on the temperature

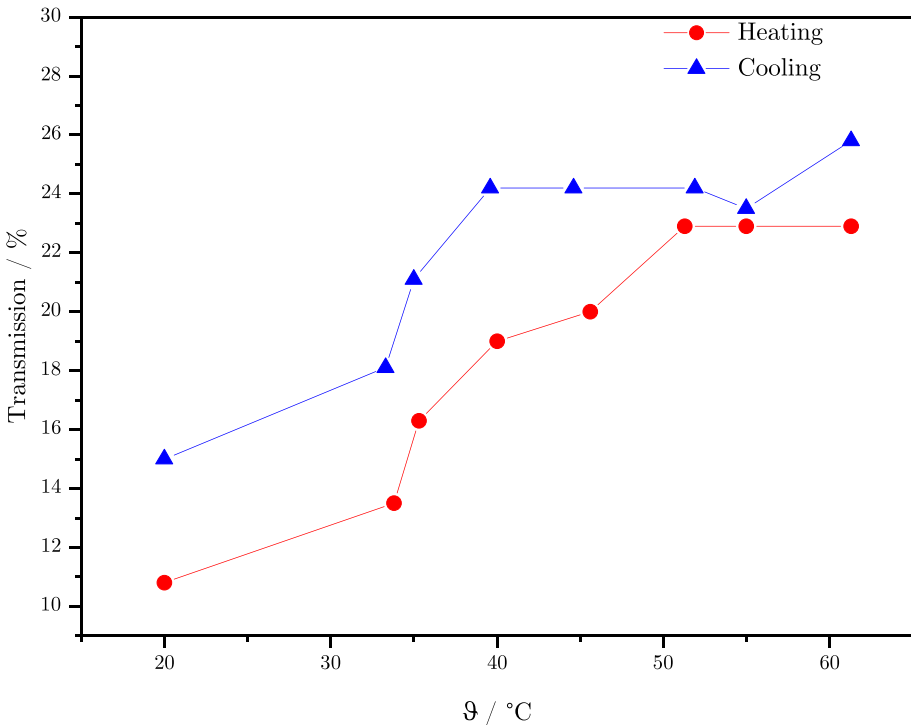


**Fig. 13** Transmission measurements of  $[Fe(atrz)_3](2 ns)_2$  in PAN with varying temperatures

spectrum of the composite. This is another indication for a successful implementation of the complex into the polymer.

The UV/VIS spectra displayed in Fig. 11b showed that both the complex and the PCC film had an absorption maximum at 525 nm at room temperature. This absorption maximum flattened in both cases as the samples were heated up to 373 K. This can be explained by the SCO properties of the used complex. To further analyse the SCO behavior, magnetic measurements were also performed in this case, as shown in Fig. 12.

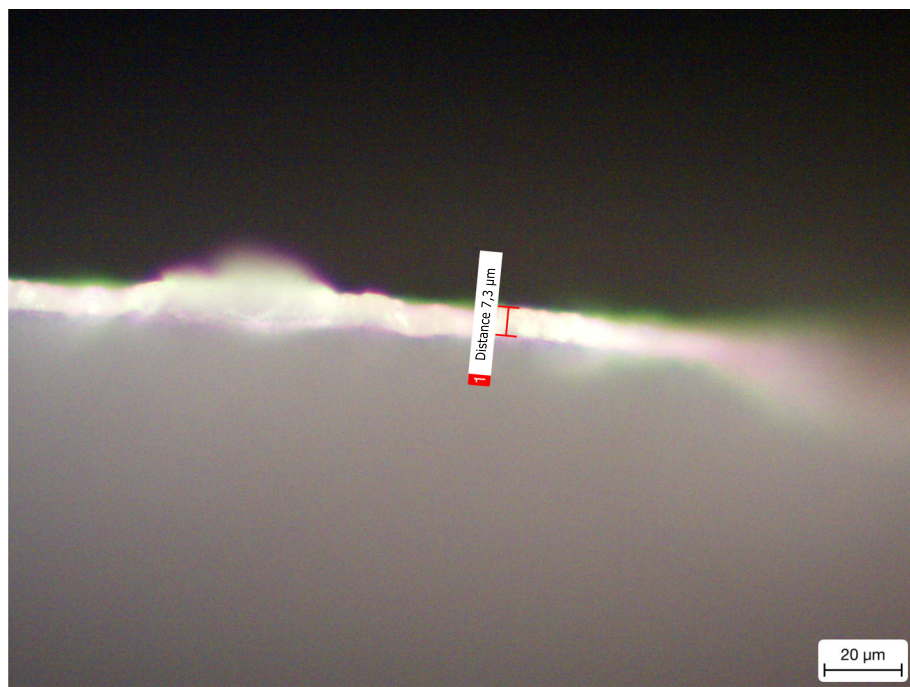


**Fig. 14** Microscopic image of  $[\text{Fe}(\text{atrz})_3](2 \text{ ns})_2$  in PAN

The base powder sample of  $[\text{Fe}(\text{atrz})_3](2 \text{ ns})_2$  shows an ideal SCO with a pronounced hysteresis loop. In the case of the PAN foil with  $[\text{Fe}(\text{atrz})_3](2 \text{ ns})_2$ , the profiles of the curves in the cooling and heating regimes have a different shape. It is believed that this characteristic behavior may be due to the dilution of the magnetic response by the matrix and/or the disruption of cooperative processes in the polymer complex composite. This is confirmed by a second measurement with a stronger magnetic field.

The used complex has also a characteristic pink color at room temperature and changed to white while heating. This obtained composite foil also got colorless while heating and seems to get more transparent as well. Therefore, the change in the transmission of light (520 nm) during heating and also cooling of the material was also studied in this case. The measurement in Fig. 13 revealed hysteresis-like behaviour of the obtained PCC thin film.

The transmission measurement showed an increase while heating and a decrease while cooling. Thereby, it was also possible to see that heating at the higher temperature for longer time also lead to a slight additional increase of the transmission. Similar behavior was also observed during cooling. This is why cooling was also observed in this case. The material showed a complete switching back after a certain time at room temperature. This can be explained by an interaction between the PAN and the complex. In total the composite thin film started with a transmission of 10.8 % of the applied laser light and came to a maximum of 25.8 % by heating. According to this, an increase of 15 % of the transmission was possible due to the SCO of the used complex, which represents a higher difference before and after the heating then in the case of  $[\text{Fe}(\text{atrz})_3]\text{Cl}_{1.5}(\text{BF}_4)_{0.5}$  in PS.

To further analyze the thin film, an optical microscope was used to determine the thickness of it. A picture of it is shown in Fig. 14 and it was possible to determine that the thin film had an average thickness of roughly  $7 \mu\text{m}$ .

## 4 Conclusion

We synthesized two different triazole complexes and used two different methods of obtaining polymer complex composite thin films. In both approaches Mössbauer spectroscopy was used to successfully confirm the implementation of the complex into the polymer. Thereby, the approach with drop casting and an insoluble complex showed a slight increase of the the  $\text{Fe}^{\text{II}}$  HS which could be explained by occurring side reactions. The second approach in which the complex was soluble, showed no change in the distribution of the spin state distribution in the Mössbauer spectrum after the implementation. Therefore, there must have been less interaction between the polymer and the complex than in the first approach. The Mössbauer spectra showed furthermore that no oxidation happened during the implementation of the complexes. In both cases, the measured IR spectra also indicated a successful implementation. Additionally, the measured UV/VIS spectra before and after implementation showed that both the prepared complexes and the thin film composites exhibited SCO properties. Due to the fact that the composites already showed a change in their optical transmission due to the SCO which was visible to the eye, appropriate measurements were carried out. These measurements proved that the obtained thin film composite materials increased their transmission due to the spin crossover effect. It was further shown that the thin films that were made with the doctor blade method were more efficient in this regard.  $[\text{Fe}(\text{atrz})_3](2\text{ ns})_2$  in PAN thin film showed a higher change in transmission than  $[\text{Fe}(\text{atrz})_3]\text{Cl}_{1.5}(\text{BF}_4)_{0.5}$  in PS. This can be explained by several reasons. One could be the remarkable difference in the layer thickness of the obtained PCCs. Thereby it is also notable that the complex of the  $[\text{Fe}(\text{atrz})_3](2\text{ ns})_2$  in PAN thin film was in solution before it was dried. The layer thickness of the approach with drop casting could potentially be decreased by applying the same amount of suspension on a bigger surface before drying. In conclusion and with regard to material for polymer-based optical waveguides, it can be said that the doctor blade method potentially enables thinner PCC materials. This will lead to higher transmission values after implemented SCO materials exhibit their switching behavior. Ongoing investigations could optimize the transmission difference after the SCO and also include other possible stimuli. Therefore, different concentrations of the complexes could be tested. This could lead to optimal functionalized waveguides for sensing applications and on top of that to low-cost sensor networks for distributed measurement, in the future [12–14].

**Acknowledgements** We thank the Nihei Laboratory of the Graduate School of Pure and Applied Sciences of the University of Tsukuba for the elemental analysis measurements. We furthermore thank the Deutsche Forschungsgemeinschaft (DFG), the Hannover School for Nanotechnology (HSN).

**Author Contributions** MSK & JB: main manuscript, general concept formal analysis, validation. Y.D. analysis & Figs. 1, 2, 7, 13, J.P. analysis, A.G., A.S. experiment Setup, data analysis, D.M.: analysis and Figs. 8 & 14, C.R. & M.P.: analysis and Figs. 6 & 12. MSK, AR, JB experiments, B.R., R.F.S., F.R.: supervision and project administration. All authors reviewed manuscript.

**Funding** Open Access funding enabled and organized by Projekt DEAL. The authors acknowledge financial support from the German Research Foundation DFG (German Research Foundation, Project ID RE 1627/13-1 and RO 3471/23-1). A.G. and B.R. also acknowledge financial support from the German Research Foundation (DFG) under Germany's Excellence Strategy within the Cluster of Excellence PhoenixD (EXC 2122, Project ID 390833453)

**Data Availability** No datasets were generated or analysed during the current study.

## Declarations

**Ethical approval** Not applicable

**Competing interests** The authors declare no competing interests.

**Open Access** This article is licensed under a Creative Commons Attribution 4.0 International License, which permits use, sharing, adaptation, distribution and reproduction in any medium or format, as long as you give appropriate credit to the original author(s) and the source, provide a link to the Creative Commons licence, and indicate if changes were made. The images or other third party material in this article are included in the article's Creative Commons licence, unless indicated otherwise in a credit line to the material. If material is not included in the article's Creative Commons licence and your intended use is not permitted by statutory regulation or exceeds the permitted use, you will need to obtain permission directly from the copyright holder. To view a copy of this licence, visit <http://creativecommons.org/licenses/by/4.0/>.

## References

1. Sugahara, A., Kamebuchi, H., Okazawa, A., Enomoto, M., Kojima, N.: Control of spin-crossover phenomena in one-dimensional triazole-coordinated iron (II) complexes by means of functional counter ions. *Inorganics* **5**(3), 50 (2017)
2. Renz, F.: Physical and chemical induced spin crossover. In: *Journal of Physics: Conference Series*, vol. 217, p. 012022. IOP Publishing (2010)
3. Roubeau, O.: Triazole-based one-dimensional spin-crossover coordination polymers. *Chem.-A Eur. J.* **18**(48), 15230–15244 (2012)
4. Lavrenova, L.G., Yudina, N.G., Ikorskii, V.N., Varnek, V.A., Oglezneva, I.M., Larionov, S.V.: Spin-crossover and thermochromism in complexes of iron (II) iodide and thiocyanate with 4-amino-1, 2, 4-triazole. *Polyhedron* **14**(10), 1333–1337 (1995)
5. Varnek, V., Lavrenova, L.: Mössbauer study of the influence of ligands and anions of the second coordination sphere in Fe (II) complexes with 1, 2, 4-triazole and 4-amino-1, 2, 4-triazole on the temperature of the 1 a 1 to 5 t 2 spin transitions. *J. Struct. Chem.* **36**(1), 104–111 (1995)
6. Dirtu, M.M., Neuhausen, C., Naik, A.D., Rotaru, A., Spinu, L., Garcia, Y.: Insights into the origin of cooperative effects in the spin transition of  $[\text{Fe}(\text{NH}_2\text{trz})_3](\text{NO}_3)_2$ : The role of supramolecular interactions evidenced in the crystal structure of  $[\text{Cu}(\text{NH}_2\text{trz})_3](\text{NO}_3)_2 \cdot \text{H}_2\text{O}$ . *Inorg. Chem.* **49**(12), 5723–5736 (2010)
7. Vinogradova, K., Andreeva, A.Y., Pishchur, D., Bushuev, M.: Spin transition in heteroanion complexes in the  $\text{Fe}^{2+}$ -4-Amino-1, 2, 4-Triazole-system. *J. Struct. Chem.* **61**(9), 1380–1389 (2020)
8. Khan, M.S., Farooq, H., Wittmund, C., Klimke, S., Lachmayer, R., Renz, F., Roth, B.: Polymer optical waveguide sensor based on Fe-Amino-Triazole complex molecular switches. *Polymers* **13**(2), 195 (2021)
9. Kilic, M.S., Brehme, J., Pawlak, J., Tran, K., Bauer, F.W., Shiga, T., Suzuki, T., Nihei, M., Sindelar, R.F., Renz, F.: Incorporation and deposition of spin crossover materials into and onto electrospun nanofibers. *Polymers* **15**(10), 2365 (2023)
10. Zhao, T., Cuignet, L., Dirtu, M.M., Wolff, M., Spasojevic, V., Boldog, I., Rotaru, A., Garcia, Y., Janiak, C.: Water effect on the spin-transition behavior of Fe (ii) 1, 2, 4-triazole 1D chains embedded in pores of MCM-41. *J. Mater. Chem. C* **3**(30), 7802–7812 (2015)
11. Koningsbruggen, P.J., Garcia, Y., Codjovi, E., Lapouyade, R., Kahn, O., Fournes, L., Rabardel, L.: Non-classical Fe II spin-crossover behaviour in polymeric iron (II) compounds of formula  $[\text{Fe}(\text{NH}_2\text{trz})_3] \times 2 \times \text{H}_2\text{O}$  (NH<sub>2</sub> trz = 4-amino-1, 2, 4-triazole; x = derivatives of naphthalene sulfonate). *J. Mater. Chem.* **7**(10), 2069–2075 (1997)
12. Rahlves, M., Günther, A., Rezem, M., Roth, B.: Polymer-based transmission path for communication and sensing applications. *J. Lightwave Technol.* **37**(3), 729–735 (2018)
13. Kelb, C., Rahlves, M., Reithmeier, E., Roth, B.: Realization and performance of an all-polymer optical planar deformation sensor. *IEEE Sens. J.* **15**(12), 7029–7035 (2015)
14. Rezem, M., Günther, A., Roth, B., Reithmeier, E., Rahlves, M.: Low-cost fabrication of all-polymer components for integrated photonics. *J. Lightwave Technol.* **35**(2), 299–308 (2017)

**Publisher's Note** Springer Nature remains neutral with regard to jurisdictional claims in published maps and institutional affiliations.



## Authors and Affiliations

Maximilian Seydi Kilic<sup>1</sup> · Jules Brehme<sup>1,2,3</sup> · Yves Deja<sup>4</sup> · Justus Pawlak<sup>1,3</sup> · Axel Günther<sup>4,5</sup> · Arthur Sander<sup>1</sup> · Dietrich Müller<sup>2</sup> · Antonia Renz<sup>1</sup> · Cyril Rajnak<sup>6</sup> · Michaela Polášková<sup>7</sup> · Bernhard Roth<sup>4,5</sup> · Ralf Franz Sindelar<sup>2,3</sup> · Franz Renz<sup>1,3</sup>

Jules Brehme  
jules.brehme@acd.uni-hannover.de

Yves Deja  
yves.deja@hot.uni-hannover.de

Justus Pawlak  
justus.pawlak@acd.uni-hannover.de

Axel Günther  
axel.guenther@hot.uni-hannover.de

Arthur Sander  
arthur.sander@acd.uni-hannover.de

Dietrich Müller  
dietrich.mueller@hs-hannover.de

Antonia Renz  
antonia.renz@hblva17.ac.at

Cyril Rajnak  
cyril.rajnak@ucm.sk

Michaela Polášková  
michaela.polaskova@upol.cz

Bernhard Roth  
bernhard.roth@hot.uni-hannover.de

Ralf Franz Sindelar  
ralf.sindelar@hs-hannover.de

Franz Renz  
franz.renz@acd.uni-hannover.de

<sup>1</sup> Institute of Inorganic Chemistry, Leibniz University Hannover, Callinstrasse 9, 30167 Hannover, Lower Saxony, Germany

<sup>2</sup> Electrospinning Laboratory, Hochschule Hannover, Ricklinger Stadtweg 120, 30519 Hannover, Lower Saxony, Germany

<sup>3</sup> Hannover School for Nanotechnology, Laboratory for Nano and Quantumengineering, Schneiderberg 39, 30167 Hannover, Lower Saxony, Germany

<sup>4</sup> Hannover Centre for Optical Technologies, Leibniz University Hannover, Nienburger Strasse 17, 30167 Hannover, Lower Saxony, Germany

<sup>5</sup> Cluster of Excellence PhoenixD (Photonics, Optics, and Engineering-Innovation Across Disciplines), Leibniz University Hannover, Welfengarten 1A, 30167 Hannover, Lower Saxony, Germany

<sup>6</sup> Department of Chemistry, University of SS Cyril and Methodius, Námestie Jozefa Herdu 577, Trnava 91701, Slovakia

<sup>7</sup> Czech Advanced Technology and Research Institute (CATRIN), Palacký University Olomouc, Křížkovského 511/8, Olomouc 77900, Czech Republic